

# Dihydroxyterephthalate—A Trojan Horse PET Cunit for Facile Chemical Recycling

Ting-Han Lee, Michael Forrester, Tung-ping Wang, Liyang Shen, Hengzhou Liu, Dhananjay Dileep, Baker Kuehl, Wenzhen Li, George Kraus, and Eric Cochran\*

Here, low-energy poly(ethylene terephthalate) (PET) chemical recycling in water: PET copolymers with diethyl 2,5-dihydroxyterephthalate (DHTE) undergo selective hydrolysis at DHTE sites, autocatalyzed by neighboring group participation, is demonstrated. Liberated oligomeric subchains further hydrolyze until only small molecules remain. Poly(ethylene terephthalate-*stat*-2,5-dihydroxyterephthalate) copolymers were synthesized via melt polycondensation and then hydrolyzed in 150–200 °C water with 0–1 wt% ZnCl<sub>2</sub>, or alternatively in simulated sea water. Degradation progress follows pseudo-first order kinetics. With increasing DHTE loading, the rate constant increases monotonically while the thermal activation barrier decreases. The depolymerization products are ethylene glycol, terephthalic acid, 2,5-dihydroxyterephthalic acid, and bis(2-hydroxyethyl) terephthalate dimer, which could be used to regenerate virgin polymer. Composition-optimized copolymers show a decrease of nearly 50% in the Arrhenius activation energy, suggesting a 6-order reduction in depolymerization time under ambient conditions compared to that of PET homopolymer. This study provides new insight to the design of polymers for end-of-life while maintaining key properties like service temperature and mechanical properties. Moreover, this chemical recycling procedure is more environmentally friendly compared to traditional approaches since water is the only needed material, which is green, sustainable, and cheap.

## 1. Introduction

Most petroleum-derived plastics like poly(ethylene terephthalate) (PET) are long-lived, resulting in “white pollution” due to their nondegradable characteristics and leakage into the environment due to inappropriate waste management practices.<sup>[1,2]</sup> Since its adoption by Pepsico for use in bottles in the 1970s,<sup>[3]</sup> PET has surpassed glass and metal as the dominant packaging material, accounting for about 6% of the global plastic market share.<sup>[4]</sup> This success has been by its low cost, high strength-to-weight ratio, impact strength, optical clarity, chemical resistance, and barrier properties. In 2021 alone, ≈81 million metric tons of PET were produced, with market forecasters anticipating 115 million tons by 2028, driven by the rising global population and attendant increase in food consumption.<sup>[5]</sup> This is accompanied by the increased production of its precursors terephthalic acid (TPA) and ethylene glycol (EG), mostly from petroleum resources. In spite of highly visible bottle recycling efforts, far less than half of PET is recycled; moreover, even recycled PET is often landfilled, with only a paltry 7% used for bottle-to-bottle recycling.<sup>[6]</sup> Ultimately, the quality of all


mechanically recycled PET becomes unsuitable for use such that the landfill and/or the environment are the terminal destinations. More than 8 million tons of plastics leak into the ocean each year, and the mass of all plastic waste is projected to exceed that of fish by 2050.<sup>[6]</sup> Even though PET has a higher recycling rate than any other type of plastic, its environmental leakage rates were about 10% of market inputs in 2018.<sup>[7]</sup>

Since the structure of PET makes it resistant to natural degradation and energy intensive for chemical recycling, it is imperative to establish new strategies for PET and PET-like materials designed for closed-loop circularity due to these ecological and economic considerations. Today, PET is reused almost exclusively via primary or secondary recycling, complex physical processes that involve sorting, cleaning, grinding, melting, and reforming.<sup>[8]</sup> The associated energy consumption is process dependent, ranging from 8 to 55 MJ kg<sup>-1</sup>.<sup>[9]</sup> Moreover, there is a notable deterioration of product performance due to

T.-H. Lee, M. Forrester, T.-p. Wang, L. Shen, H. Liu, D. Dileep, B. Kuehl, W. Li, E. Cochran

Department of Chemical and Biological Engineering  
Iowa State University  
Ames, IA 50011, USA  
E-mail: ecochran@iastate.edu

G. Kraus  
Department of Chemistry  
Iowa State University  
Ames, IA 50011, USA

 The ORCID identification number(s) for the author(s) of this article can be found under <https://doi.org/10.1002/adma.202210154>.

© 2023 The Authors. Advanced Materials published by Wiley-VCH GmbH. This is an open access article under the terms of the Creative Commons Attribution-NonCommercial License, which permits use, distribution and reproduction in any medium, provided the original work is properly cited and is not used for commercial purposes.

DOI: 10.1002/adma.202210154

degradation, oxidation, contamination, and altered molecular weight distribution.<sup>[8]</sup>

Tertiary recycling, known commonly as chemical recycling or chemolysis, promises the recovery of virgin monomers that can be used to regenerate brand-new plastics, even from highly damaged and contaminated feedstocks. Multiple approaches for PET chemolysis have been considered including glycolysis, alcoholysis, and hydrolysis.<sup>[10]</sup> Hydrolysis uses aqueous solutions with acidic, alkaline, or neutral catalysts, whereas glycolysis and alcoholysis use glycols or alcohols, respectively. Other approaches such as aminolysis and ammonolysis use aqueous amine solutions or ammonia, but these are seldom considered due to the lack of product application.

As the simplest and oldest approach to PET depolymerization, glycolysis has been studied thoroughly. Generally, EG is used to attain the precursor bis(hydroxyethyl) terephthalate (BHET) for subsequent PET regeneration. Besides temperature and time, various catalysts, including metal acetates, metal oxides, carbonates, sulfates, ionic liquids, and others have been investigated. Metal acetates are the most widely used with activities ordering as  $Zn^{2+} > Pb^{2+} > Mn^{2+} > Co^{2+}$  and BHET yields ranging 70–100%.<sup>[11]</sup> Imran et al. used pure oxides and mixed-oxide spinel as catalysts and indicated better efficiency compared to single oxides due to higher surface area and acid site concentration. The type of metal cation, coordination geometry (tetrahedral or octahedral), and the spinel geometry (tetragonal or cubic) affected yield.<sup>[12]</sup> Al-Sabagh et al. studied glycolysis using Cu- and Zn-acetate-containing ionic liquids as catalysts which evidently retained activity for up to six reuses.<sup>[13]</sup> Moreover, product recovery from ionic liquid catalyzed processes was simpler compared to conventional catalysts like metal acetates. Microwave-assisted glycolysis of PET has gained considerable attention due to the 300 s time scale required to achieve nearly complete conversion, albeit at energy requirements near  $60 \text{ MJ kg}^{-1}$ .<sup>[14,15]</sup>

Alcoholysis involves the degradation of PET in an alcoholic medium under high temperature and pressure, with methanolysis having drawn the most attention over recent years. It can proceed under three forms: liquid (conventional), super-heated (vapor), or supercritical.<sup>[16–18]</sup> The conventional process uses the same catalysts as glycolysis, whereas the super-heated pathway leads to a lower decomposition rate but has higher tolerance for contaminated PET. The supercritical process achieves significantly higher PET decomposition rates without catalyst, albeit at the expense of severe reaction conditions ( $T > 240 \text{ }^\circ\text{C}$ ,  $P > 8 \text{ MPa}$ ).

Hydrolysis of PET can be performed with acids like  $\text{H}_2\text{SO}_4$  and  $\text{HNO}_3$ , alkalis like NaOH and KOH, or neutral materials including metal acetates, phase transfer agents, or hydrotalcite in aqueous or nonaqueous media.<sup>[19]</sup> Campanelli et al. demonstrated complete depolymerization to monomers in excess water at  $265 \text{ }^\circ\text{C}$  for 2 h.<sup>[20]</sup> Güçlü et al. carried out neutral hydrolysis of PET with different amounts of water and different catalysts in xylene. They concluded that xylene facilitated both depolymerization and subsequent monomer purification.<sup>[21]</sup> Mancini and Zanin used 7.5 M sulfuric acid to reach 80–90% depolymerization over 4 days at  $100 \text{ }^\circ\text{C}$  and in 5 h at  $135 \text{ }^\circ\text{C}$ .<sup>[22]</sup> Karayannidis et al. conducted alkaline hydrolysis at  $120\text{--}200 \text{ }^\circ\text{C}$  with aqueous NaOH solutions to yield high purity disodium

terephthalate.<sup>[23]</sup> Recently, Wang et al. showed nearly quantitative hydrolysis of PET at  $180 \text{ }^\circ\text{C}$  after 8 h in aqueous 70 wt%  $\text{ZnCl}_2$  solution.<sup>[24]</sup>

While these recycling pathways are fascinating and hold great promise, they are still too resource-intensive to merit large-scale implementation, all requiring some combination of harsh conditions, time, and separations with energy consumption on the order of  $60 \text{ MJ kg}^{-1}$  or higher.<sup>[24–26]</sup> In practice, glycolysis products comprise a significant number of oligomers besides BHET, imposing separations challenges that impede commercial adoption.<sup>[27]</sup> While methanolysis produces relatively pure dimethyl terephthalate (DMT) and EG, it requires relatively high temperature and pressure. Moreover, most PET manufacturing is based on TPA rather than DMT, the conversion of which would impose further processing costs.<sup>[23]</sup> Hydrolysis is the only method to directly recover TPA and EG from PET, but the harsh catalytic conditions would cause high corrosion to the facility and generate undesirable inorganic salts due to the concentrated acidic or basic solution used.<sup>[28]</sup>

Thus in general, chemolytic processes all require some combination of organic solvents, concentrated acidic/basic solutions, catalysts, and/or extreme conditions like high temperature or pressure. These requirements significantly increase the capital cost combined with the environmental cost.<sup>[29]</sup> Moreover, the separation and purification of products like BHET is difficult. As a result, further efforts to achieve resource-efficient and environmentally benign methods for PET chemical recycling are indicated.

Herein, we introduce a family of PET copolymers embedded with a “Trojan Horse” (TH) count that enables depolymerization under far milder conditions as illustrated in **Figure 1**. Our previous work with poly(1,5 dimethoxy-2,6 ethylene naphthalate) showed that unlike other poly(ethylene naphthalates) with thermal stability to over  $400 \text{ }^\circ\text{C}$ , this material underwent rapid chain scission in both aerobic and anaerobic environments near  $200 \text{ }^\circ\text{C}$ .<sup>[30]</sup> Evidently, the ortho-substituents coordinated to facilitate decomposition reactions through an autocatalytic process known as “anchimeric assistance” or “neighboring group participation” (NGP).<sup>[31]</sup> In fact, Kaplan and Sawodny used a similar substitution pattern to demonstrate complexation with metals in a series of polyesters based on 2,5-dihydroxyterephthalic acid.<sup>[32]</sup> These authors noted decreases in the thermal stability as measured by TGA under  $\text{N}_2$  by up to  $100 \text{ }^\circ\text{C}$  depending on the complexed metal cation. Based on these observations, we hypothesized that chemically reversible NGP-activated reactions in terephthalate analogs like 2,5-dihydroxyterephthalate could be exploited to insert a chink into the armor of otherwise chemically resilient polymers. By copolymerizing with  $\leq 20 \text{ mol}\%$  DHTE, PET retains or improves upon key performance features while exhibiting drastically enhanced sensitivity to hydrolysis under selective conditions. DHTE can be synthesized readily from biobased succinic acid (SA), a diacid sugar fermentation product recognized as one of the top 12 value-added platform chemicals derived from biomass by US Department of Energy (DOE).<sup>[33–35]</sup> It should be noted that SA along with other aliphatic-like diacids, including adipic, sebacic, and maleic acids, have been used as comonomers to modify the properties of PET, especially in terms of its crystallinity and hydrophobicity in order to gain biodegradability.<sup>[36]</sup> However,

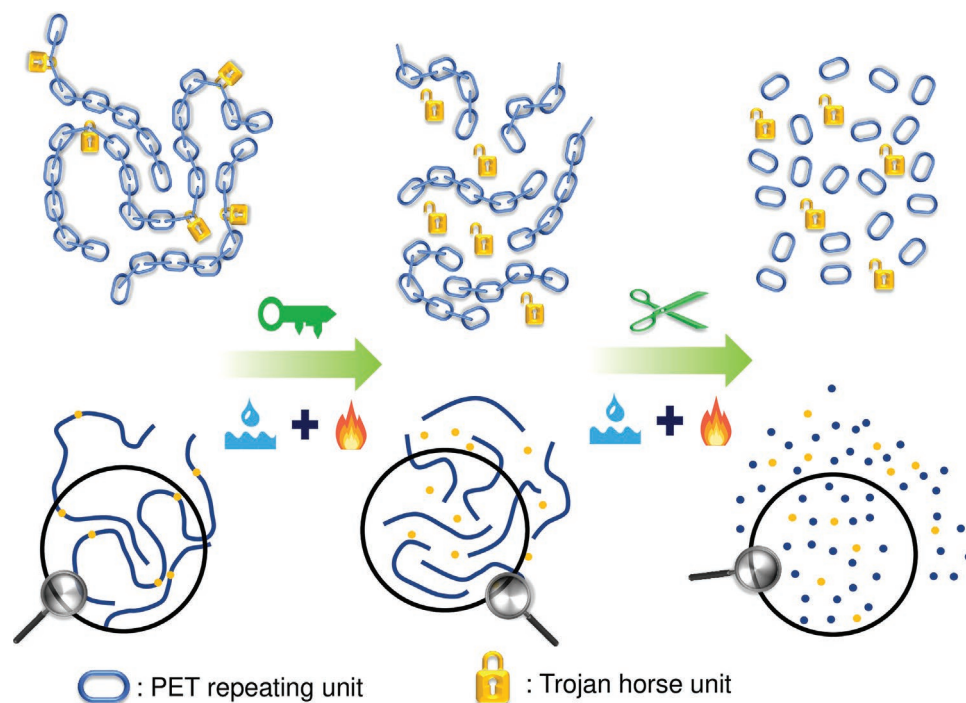


**Figure 1.** Conceptual illustration of the Trojan-Horse paradigm for PET chemical recycling.

while the introduction of these chemicals into PET polymer backbone increased its degradability, they also reduced the thermal and mechanical properties. Here, appropriately chosen TH counts could both retain the high performance of PET due to their aromatic structure while introducing degradability due to NGP. In this work, abundant and inexpensive water served as both solvent and reactant. The PET copolymers were depolymerized with zinc-based catalysts through selective cleavage of C-O bonds due to the metal ion coordination with ester and phenolic groups. Additionally, we found appreciable activity even without catalyst and in a simulated marine environment. The depolymerization products, TPA and 2,5-dihydroxyterephthalic acid (DHTE), readily precipitated from water at room temperature. This strategy provides several orders of magnitude improvement of relatively inefficient chemical deconstruction

reaction and high precursor recovery while retaining the thermal and mechanical performance of legacy PET.

## 2. Results and Discussion

The characteristics of the materials that were synthesized for this study are summarized in **Table 1**. The sample codes of the copolymers are denoted as Poly(ethylene terephthalate-*stat*-2,5-dihydroxyterephthalate)*X* (*X*), where *X* represents the mole fraction % of DHTE units relative to the total amount of diester and diacid.

PET and PEDHT copolymers were synthesized by a two-step polymerization similar to the industrial manufacturing process. The first step is monomer preparation

**Table 1.** Composition and reaction conditions of PET and PEDHT copolymers.

Sample code <sup>a)</sup>	Feed ratio TPA/DHTE/EG [equiv.] <sup>b)</sup>	Polycondensation				
		temp./time <sup>c)</sup> [°C h <sup>-1</sup> ]	Insoluble fraction <sup>d)</sup> [%]	Soluble fraction $M_n$ <sup>e)</sup> [kDa]	Soluble fraction $M_w$ <sup>f)</sup> [kDa]	Soluble fraction [ $\bar{D}$ ] <sup>g)</sup>
PET	1/0/10	240/8	0.0	15.7	31.3	2.00
PEDHT5	0.95/0.05/10	240/2.5	3.9	11.8	51.5	4.35
PEDHT10	0.9/0.1/10	240/2	5.4	11.3	58.2	5.13
PEDHT20	0.8/0.2/10	240/1.75	11.3	12.2	72.0	5.88

<sup>a)</sup>Sample code: PEDHTX, X = mol% of dihydroxyterephthalate repeat unit; <sup>b)</sup>Equivalents of terephthalic acid (TPA) & diethyl dihydroxyterephthalate (DHTE) on a 10 equiv. basis of ethylene glycol (EG); <sup>c)</sup>The esterification/transesterification reaction was carried out at 220 °C for 5h and bis-hydroxy ester monomer conversion of each precursor is  $\geq 99\%$ , which was determined by gas chromatography-mass spectrometry; <sup>d)</sup>Insoluble fraction by dissolving sample in phenol/1,1,2,2-tetrachloroethane (60/40, v/v) at 120 °C for 16 h; <sup>e)</sup>Number-average molecular weight; <sup>f)</sup>Weight-average molecular weight; <sup>g)</sup>Dispersity calculated by  $M_w/M_n$ . The molecular weights were determined by GPC in 1,1,1,3,3,3-hexafluoro-2-propanol solution with Poly(methyl methacrylate) standards.

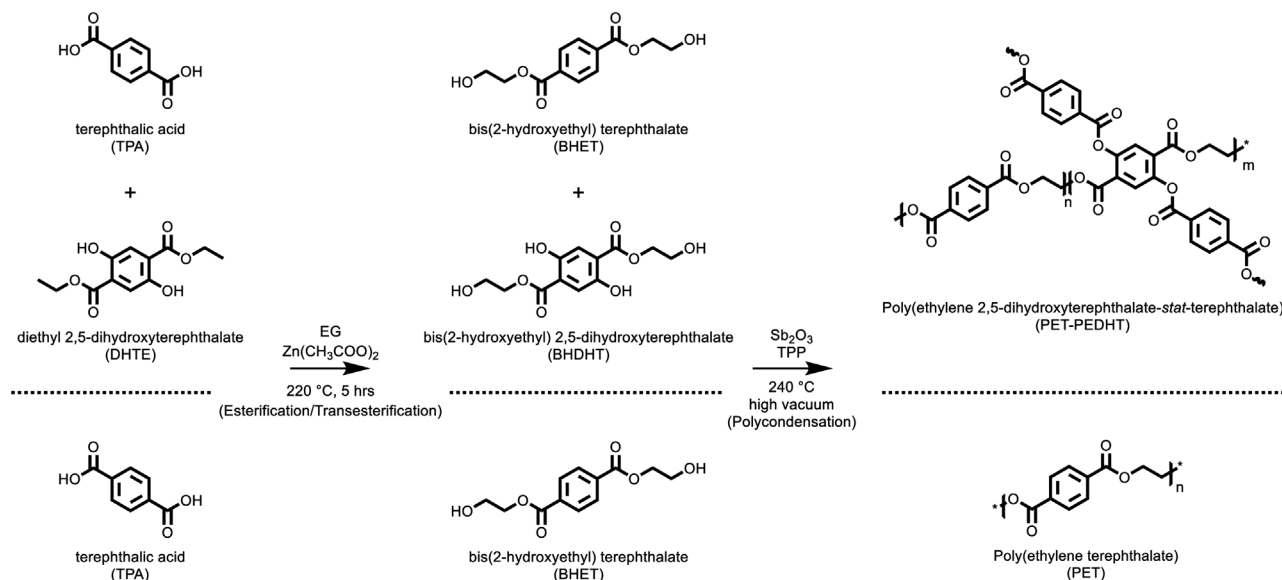


**Figure 2.** Step-growth polycondensation of pure PET and PET-PEDHT copolymer via a two-step polymerization.

(esterification/transesterification), in which diacid/di-ethyl ester is converted to bis-hydroxy ester. The conversion reached >99% within 5 h using excess EG without side reactions, as shown in Figure S1, Supporting Information. Following the completion of monomer preparation and distillation to remove excess EG, the bis-hydroxy ester was mixed with additional catalyst and converted into polyester through transesterification under dynamic vacuum. It should be noted that viscosity was higher during the polymerization of PEDHT copolymers compared to pure PET. Therefore, this reduced the reaction time and further caused limitations on the growth of the polymer chain. In solvating the polymers for GPC analysis, we noted that a portion of the PEDHT specimens was insoluble. Soluble PEDHT fractions had number-average molecular weights comparable to pure PET. The dispersity ( $D$ ) of PEDHT copolymers exceeded over two times that typically associated with a polycondensation material, and  $D$  increases with DHTE content (Figure S2, Supporting Information). The increased viscosity, insoluble fraction, and elevated dispersity are ascribed to the permanent covalent network that formed due to the chain extension, branching, and/or cross-linking reactions via reaction of phenolic and carboxylic/ester, as indicated in Figure 2. The insoluble fraction (Table 1) results indicate that the degree of cross-linking increases with DHTE content. In general, PEDHT copolymers are within the conditions required to assess the performance of these materials and well enough to make a comparison with pure PET.

In addition to solution state analyses, FTIR spectroscopy was used to analyze the microstructure of the copolymers in the solid state as shown in Figure 3. The strong absorption peaks in the region of 1714 and 1681  $\text{cm}^{-1}$  are assigned to the stretching vibration of the carbonyl group (C=O) of PET and PEDHT units, respectively, while the peaks at 1237 and 1191  $\text{cm}^{-1}$  correspond to carbonyl (C-O) stretching vibration of PET and PEDHT units, respectively. The frequency of carbonyl (C=O) stretching peak of PEDHT unit is 33  $\text{cm}^{-1}$  lower than that of PET due to the electron-withdrawing effect of the additional

phenolic groups on the aromatic ring.<sup>[37]</sup> In general, the FTIR spectra of PEDHT copolymers show different absorption peaks of C=O and C-O stretching vibration for PET and PEDHT units, respectively, and the ratio of absorption intensities ( $I_{1714}/I_{1681}$  and  $I_{1237}/I_{1191}$ ) decreases with the increase in the PEDHT unit content. Although FTIR is not well-suited to the precise quantitation of the DHTE composition, the intensity ratios observed in the spectra are consistent with the monomer feed ratios. These values are also consistent with the DHTA/TPA ratio determined via NMR after depolymerization as described below. Furthermore, it should be mentioned that the phenolic (-OH) group of DHTE was observed at 3286  $\text{cm}^{-1}$ , while there was no significant peak showing up in this region of PEDHT copolymers. This is consistent with the esterification of phenolic groups during polycondensation, resulting in a 3D network. This supports the hypothesis that the insoluble fraction

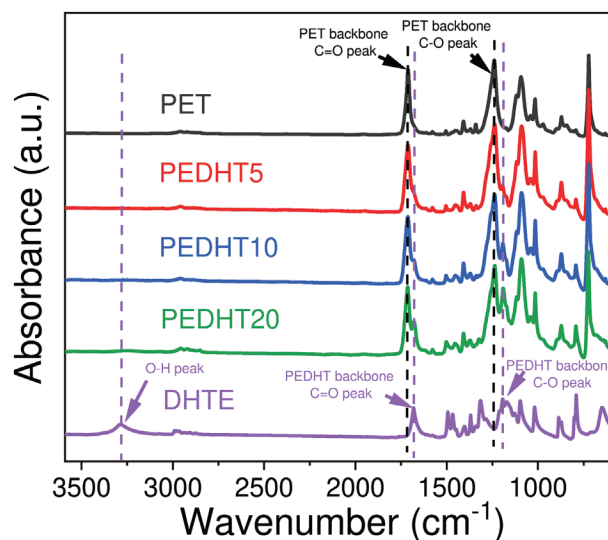


**Figure 3.** ATR-FTIR spectra of PET and PEDHT copolymers.

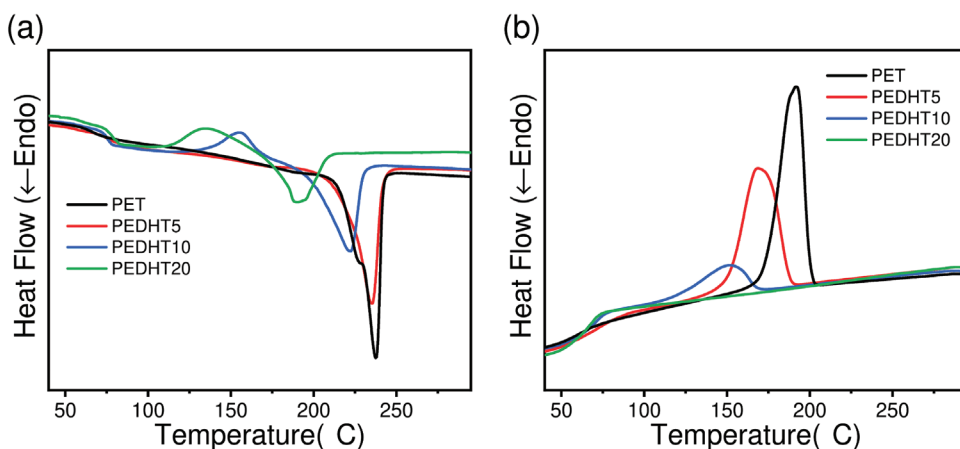


**Figure 4.** DSC thermograms of PET and PEDHT copolymers: a) second heating and b) second cooling (scan rate was 10 °C min<sup>-1</sup>).

of the copolymers is attributed to the permanent covalent network formed due to phenolic –OH esterification.<sup>[38,39]</sup>

To elucidate the effect of DHTE loading on the thermal properties of the copolymers, differential scanning calorimetry (DSC) was performed (see **Figure 4** and **Table 2**). The melting point  $T_m$  decreases monotonically with DHTE loading. This trend is observed in studies on other statistical copolymers, including polyamides, and can be attributed to the suppression of the crystal thickness resulting from the comonomer unit within the polymer chain.<sup>[40–42]</sup> In most cases, crystals are comprised solely of majority component, with the minority counts relegated to the amorphous phase. In this case, as DHTE fraction increases, the crystal thickness is suppressed due to shorter PET sequences. This depresses the melting point as anticipated by the Thompson–Gibbs equation.<sup>[43]</sup> Moreover, a similar trend is observed in melting enthalpy and degree of crystallinity, which supports the suppression effect of crystal thickness by the comonomer units. On melt recrystallization, DHTE loading also depresses the recrystallization temperature  $T_c$ , crystallization enthalpy, and the degree of crystallinity obtained. These effects are in part due to disruption of crystallizable PET sequences with DHTE defects. Additionally, suppression of chain rearrangements owing to the covalent network likely plays a role. Chain diffusivity will be increasingly attenuated with increasing DHTE composition and the attendant increase in cross-link density. Similar crystallization behavior effects have been noted in branched/cross-linked

poly(butylene terephthalate)s.<sup>[44]</sup> Turning to the amorphous phase, where the vast majority of the DHTE content evidently resides, all PEDHT copolymers show one unique  $T_g$  value via DSC, indicating a homogeneous amorphous phase. The PEDHT copolymers show  $T_g$  values 4–7 °C higher compared to PET, which is likely a consequence of the restricted segmental motion due to DHTE-mediated crosslinking.

Based on thermal property characterization, PEDHT copolymers are similar to pure PET for a wide range of practical applications since the copolymers show higher service temperature and ease-of-processing due to the improved  $T_g$  and reduced  $T_m$ , respectively, compared to PET. Additionally, we characterized the thermal stability of PEDHT copolymers using thermogravimetric analysis (TGA) (See **Figure 5** and **Table 2**). The results indicate that the thermal stability of PEDHT copolymers is similar to that of PET, while producing similar char residue and slightly higher  $T_{d,max}$  values. The enhancement of the thermal stability is attributed to the permanent covalent network formed by DHTE, which reinforces the dimensional stability of the polymer structure. In summary, the thermal analysis demonstrates that PEDHT copolymers retain thermal properties comparable to PET.

The presence of the melting behavior indicates that the copolymers are melt processable. This means PEDHT copolymers could be processed analogously to PET, that is, via injection or blow molding for commodity production. Therefore, to confirm this hypothesis, injection molding was used to

**Table 2.** Thermal transition properties of PET and PEDHT copolymers.

Sample code <sup>a)</sup>	DSC								TGA		
	$T_g$ <sup>b)</sup>	$\Delta H_{cc}$ <sup>b)</sup>	$T_{cc}$ <sup>b)</sup>	$\Delta H_c$ <sup>b)</sup>	$T_c$ <sup>b)</sup>	$\Delta H_m$ <sup>b)</sup>	$T_m$ <sup>b)</sup>	$\chi_c$ <sup>b)</sup>	$T_{d,5\%}$ <sup>c)</sup>	$T_{d,max}$ <sup>c)</sup>	$R_{1000}$ [wt%] <sup>c)</sup>
PET	71.2	N.D. <sup>d)</sup>	N.D.	43.2	191.7	38.6	237.5	27.5	404.8	442.1	16.0
PEDHT5	78.6	N.D.	N.D.	37.7	168.4	35.8	235.3	25.6	404.8	444.8	17.7
PEDHT10	75.5	8.5	155.5	10.9	150.9	30.6	222.0	21.9	391.3	442.9	16.4
PEDHT20	77.8	10.1	135.2	N.D.	N.D.	18.3	190.0	13.0	369.0	444.6	14.6

<sup>a)</sup>Sample code: PEDHTX, X = mol% of dihydroxyterephthalate repeat unit; <sup>b)</sup>Glass transition ( $T_g$ ), crystallization ( $T_c$ ), cold crystallization ( $T_{cc}$ ), and melting ( $T_m$ ) temperatures; The enthalpies ( $\Delta H_{cc}$ ,  $\Delta H_c$ , and  $\Delta H_m$ ) corresponded to each thermal transition; <sup>c)</sup> $T_{d,5\%}$ : decomposition temperatures at which the weight loss reached 5% of its initial weight;  $T_{d,max}$ : the temperature at the maximum rate of decomposition;  $R_{1000}$ : The residual mass at 1000 °C; <sup>d)</sup>Not detected by DSC.

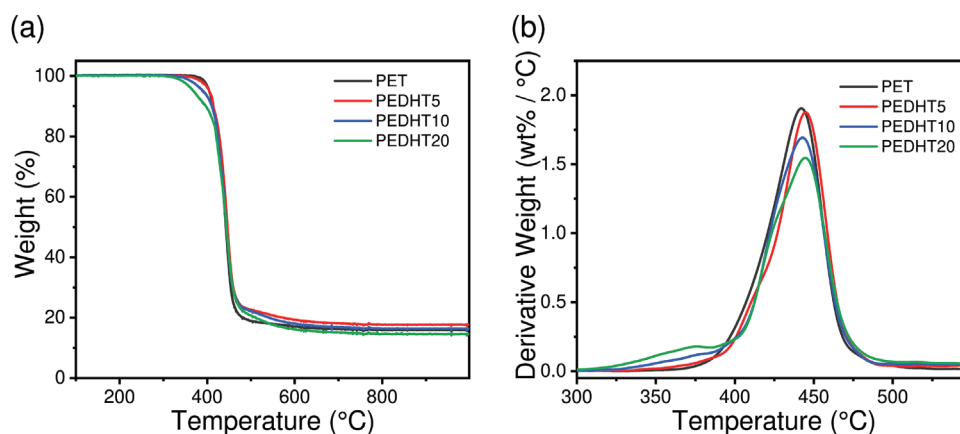


**Figure 5.** a) TGA thermograms and b) DTG curve of PET and PEDHT copolymers. Heating rate was 10 °C min<sup>-1</sup>.

process PEDHT copolymers. The injection molding conditions used for PEDHT and PET were identical; the increased PEDHT melt viscosity did not interfere with this process. Furthermore, the melting point of PEDHTs is lower, indicating that PEDHT possesses the potential to improve energy consumption during the manufacturing process and reduces thermal polymer chain degradation. However, further study on product processing is necessary to give a comprehensive understanding of PEDHT processability. The produced tensile samples were used to determine the mechanical properties, shown in **Table 3**. (see Figure S3, Supporting Information for representative stress-strain curves) The Young's modulus of PEDHT copolymers shows an increase of 40% compared to that of PET. This result can be attributed to the presence of the DHTE network, which enables the materials to withstand higher load under the same degree of deformation. Likewise, the copolymer yield strength increases from 74 to 102 MPa for  $\geq 10$  mol% DHTE loading. This observation can be attributed to the increase in the rigidity of the copolymers due to the change in the cross-link density; as this increases, the material can withstand with stronger forces before necking. Based on these effects, a similar trend is observed in the ultimate strength, which shows an improvement of 110% from 45 to 96 MPa with DHTE loading  $\geq 10$  mol%. While the cross-linking improves the rigidity and strength of the materials, elongation-at-break decreases from 358% to 23% with DHTE, changing the fracture fashion of the copolymers from ductile-to-brittle. This can result from the disruption effect of 3D network which disrupts the strain-induced crystallization and lead to material fracture, indicating a tradeoff for the increase in the stiffness of the polymer. Therefore, the mechanical

properties are tunable through DHTE content to meet a range of performance specifications.

Traditional PET hydrolysis is mediated through catalysis with acidic, basic, or heavy metal solutions. The cations attack the acyl O of the ester, which results in the shift of the electronic cloud away from the acyl C. This allows the O of H<sub>2</sub>O to attach to the activated acyl C, cleaving the polymer chain.<sup>[45]</sup> While this process is quite facile in solvated esters, the highly crystalline nature of PET severely impedes the ingress of reactive species into the solid bulk. Ostensibly, the onset of hydrolysis is relegated to the amorphous phase near the surface. In this work, we hypothesized that TH counits like DHTE would facilitate depolymerization by more rapidly releasing oligomeric subchains with far greater affinity for the aqueous phase. To test this, we conducted several depolymerization experiments varying time, temperature, and catalyst composition. The results are summarized in **Table 4** and Tables S1 and S2, Supporting Information; **Figure 6** and Figures S4 and S5, Supporting Information.

Given the demonstrated efficacy of Zn<sup>2+</sup> in the catalysis of PET hydrolysis and glycolysis,<sup>[24,46]</sup> we first determined the sensitivity of ZnCl<sub>2</sub> concentration on depolymerization kinetics comparing PET and PEDHT10 at 170 °C and 8 h. PET is quite resilient without catalyst under these conditions, losing only 16 wt% of its mass. Using the staggering 70 wt% ZnCl<sub>2</sub> employed by Wang et al.,<sup>[24]</sup> mass loss increases nearly three-fold to 47 wt% (Table 4). In comparison, uncatalyzed depolymerization of PEDHT10 realizes 67% mass loss, increasing slightly to 72 wt% with 1 wt% ZnCl<sub>2</sub>. While we mainly attribute the significant depolymerization of PEDHT10 in the absence of ZnCl<sub>2</sub> to the NGP autocatalysis afforded by the DHTE counits, we also suspect that residual Zn(CH<sub>3</sub>COO)<sub>2</sub> used in polymer

**Table 3.** Mechanical properties of PET and PEDHT copolymers.

Sample code <sup>a)</sup>	Young's modulus [MPa]	Toughness [MJ m <sup>-3</sup> ]	Yield strength [MPa]	Elongation at break [%]
PET	1040.5 ± 13.0	157.5 ± 8.2	74.1 ± 2.4	358.2 ± 14.4
PEDHT5	1477.5 ± 16.5	46.2 ± 5.8	83.5 ± 0.8	60.1 ± 7.0
PEDHT10	1449.5 ± 42.2	32.7 ± 4.0	102.3 ± 2.2	36.8 ± 4.3
PEDHT20	1491.6 ± 96.4	18.0 ± 2.0	97.7 ± 1.1	22.8 ± 1.4

<sup>a)</sup>Sample code: PEDHTX, X = mol% of dihydroxyterephthalate repeat unit.

**Table 4.** Hydrolysis degradation results of PET and PEDHT copolymers under different reaction conditions.

Sample code	ZnCl <sub>2</sub> concentration [%]	Temperature [°C]	Time [h]	Degradation conversion <sup>a)</sup> [%]
PET	0	170	8	16.3
	70	170	8	46.5
PEDHT5	0	160	8	34.4
	0	170	8	59.6
	0	180	8	81.0
	Sea water	160	8	38.1
	Sea water	170	8	66.5
	Sea water	180	8	82.0
	0	200	2	98.7
PEDHT10	0	170	8	66.9
	1	160	8	43.7
	1	170	8	72.4
	1	180	8	93.4
PEDHT20	0	150	8	21.1
	0	160	8	59.5
	0	170	8	93.6

Mass ratio of polymer to aqueous solution was 1:30; <sup>a)</sup>Degradation conversion was calculated from NMR quantitative analysis.

synthesis plays an important role.<sup>[47]</sup> The rate constants and conversions vary slightly when ZnCl<sub>2</sub> concentration increases from 0% to 1% (see Figure 6a), which suggests that a residual amount of Zn(CH<sub>3</sub>COO)<sub>2</sub> (0.004 wt% of solution) already significantly facilitates hydrolysis. The more efficient catalytic effect of Zn(CH<sub>3</sub>COO)<sub>2</sub> could be attributed to the fact that it is homogeneously distributed in the powder phase versus in solution, and also that the acetate ion is a stronger base compared to chloride ion in the solution.

Based on the 11.3 kDa molecular weight estimate for PEDHT10, a random distribution of DHTE repeat units implies that roughly 1 kDa oligomers (6–7 repeat units) are first liberated by the NGP-accelerated hydrolysis. These could be retained in the polymeric solids or lost to the supernatant. To investigate the hydrolysis products, <sup>1</sup>H-NMR and GC-MS were per-

formed, Figures S6 and S7, Supporting Information. The NMR of the solids precipitated from the aqueous solution shows the peak signal at 8.02 ppm, which indicates the four aromatic TPA protons, while the signal at 7.27 ppm corresponds to the two aromatic DHTE protons. The peak signal at 4.66 ppm is the methylene unit from the ethylene glycol linkage in BHET dimer, while the signals at 4.30 and 3.71 ppm are the terminal methylene units of BHET dimer, in accordance with the NMR result of BHET dimer reported in the literature.<sup>[48]</sup> In the case of liquid products, the peaks of 3.40 and 4.75 ppm are designated to protons of the methylene and hydroxy groups of EG, respectively. GC-MS was used to further verify the purity and the composition of the solid products, and results appear in Figure S7 and Table S3, Supporting Information. The GC-MS chromatographs show three major peaks, corresponding to three distinct molecules. The peaks with retention times of 9.48 and 12.15 min have mass spectra matching TPA and DHTE, respectively, while the peak at 11.48 min is consistent with BHET dimer. Both the yield and the purity of the solid products are over 90%. Furthermore, DHTE in the composition of the solid products is consistent with the DHTE loading inside the copolymers. Based on this analysis, we conclude that the liberated oligomers from the PEDHT subsequently undergo hydrolysis exclusively to monomers and BHET dimer.

To further understand the depolymerization of PEDHT copolymers, the mechanism should be considered. According to previous studies, the catalyst used for depolymerization will interact with the solvent (water/EG) and the ester bonds of PET to facilitate depolymerization.<sup>[13,24,49]</sup> In the case of the TH-containing PEDHT copolymers, the proposed degradation mechanism is presented in Figure 7. Water is first activated in the presence of ZnCl<sub>2</sub> and Zn(CH<sub>3</sub>COO)<sub>2</sub> via hydrogen bond interactions.<sup>[50]</sup> Next, depolymerization reactions are considered at both TH repeat units and PET repeat units. Note that the phenolic group of DHTE reacts with the hydroxy ester end group of the polymer chain to form an ester bond. We assume that the chelate forms when Zn<sup>2+</sup> of ZnCl<sub>2</sub> and Zn(CH<sub>3</sub>COO)<sub>2</sub> coordinates with the oxygen atom of the ester bond in the polymer backbone and on the TH unit. This coordination effect would allow the ester bonds to be more reactive with the hydroxide ion (OH<sup>-</sup>) of H<sub>2</sub>O as reported by Sara et al.<sup>[51]</sup> Meanwhile, electronic destabilization occurs, and the electronic cloud

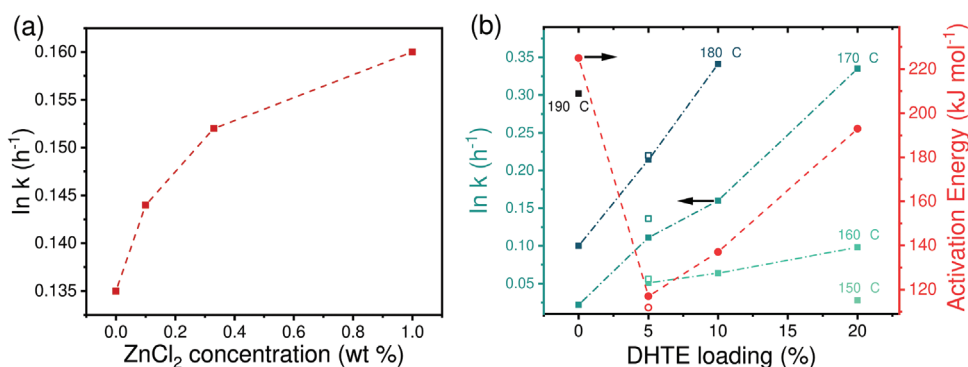


**Figure 6.** Effect of the reaction conditions on the degradation kinetics of PET and PEDHT copolymers. a)  $\ln k$  versus ZnCl<sub>2</sub> concentration of PEDHT10 at 170 °C, and b)  $\ln k$  (left axis, □) and  $E_a$  (right axis, ○) versus DHTE loading. Filled symbols are 0% ZnCl<sub>2</sub> (except for 10% loading which is 1% ZnCl<sub>2</sub>). Open symbols denote sea water experiments. Color gradient from light blue to dark blue indicates temperature from 150 to 190 °C).

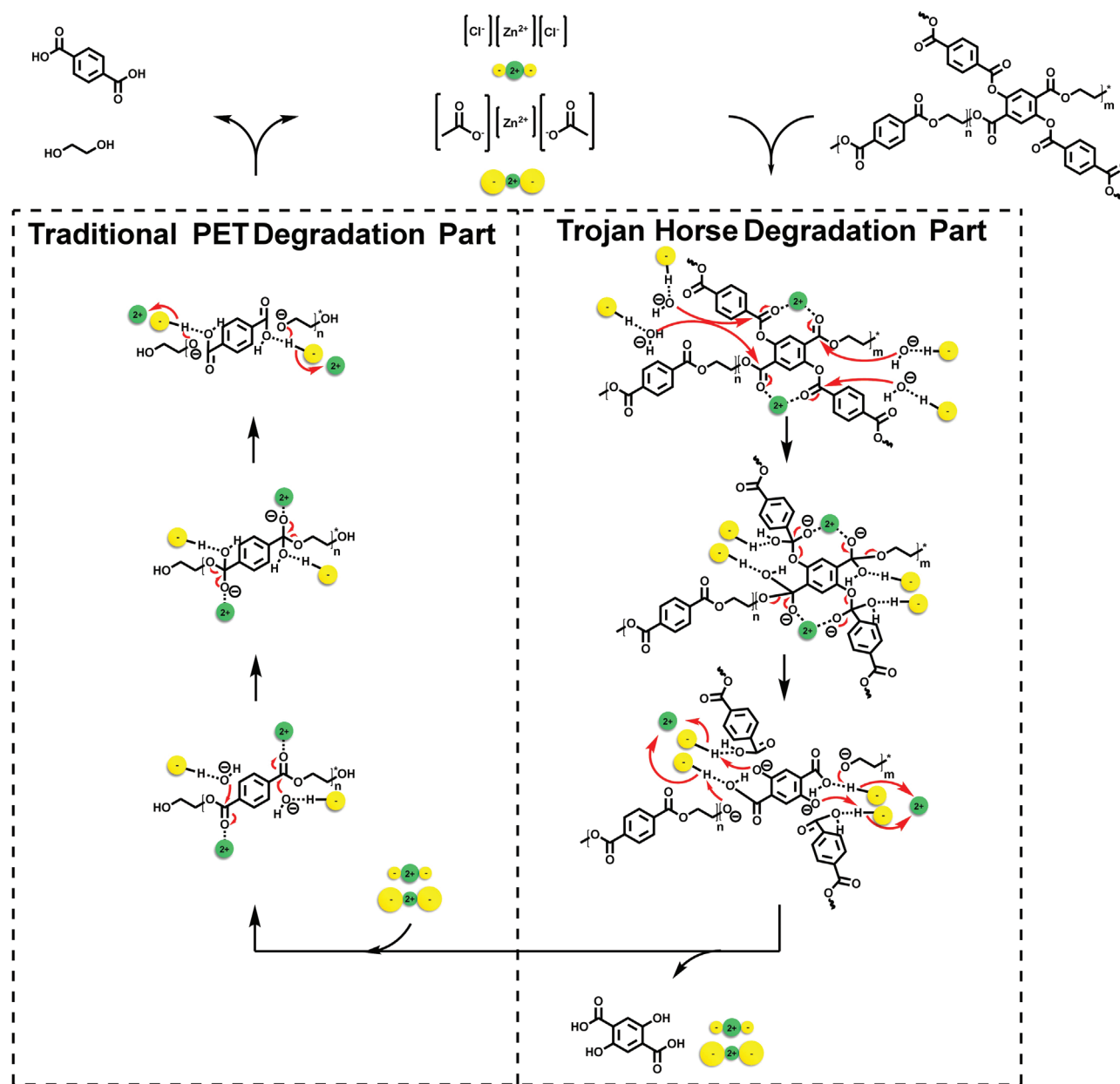


**Figure 7.** Proposed TH-unit mediated degradation mechanism in PEDHT copolymers via selective cleavage of ester bonds in the presence of Zn-based catalysts.

shifts to the oxygen atom, making the carbon atom of the ester bond to be positively charged. Then, the nucleophilic oxygen of  $\text{H}_2\text{O}$  attacks the acyl carbon of the ester bond to form carboxylic ( $-\text{COOH}$ ) end group, whereas the proton ( $\text{H}^+$ ) of  $\text{H}_2\text{O}$  reacts with the acyl-oxygen of PET to form  $\text{HOCH}_2\text{CH}_2^-$ . During this stage, the copolymers break into shorter PET chains. Afterward, the shorter chains go through a similar degradation mechanism as reported elsewhere.<sup>[13,24,50]</sup> The  $\text{Zn}^{2+}$  only coordinates with the oxygen atom of the ester bonds in the polymer chains, which displays a similar coordination effect to that of the TH component. Nonetheless, the depolymerization rate of the PET part decreases dramatically due to the absence of the chelate formation. Finally, hydrolysis of the shorter polymer chains occurs,

and oligomers, dimers, as well as monomers are generated sequentially. Based on the proposed mechanism mentioned above, the formation of the chelate due to the coordination effect between metal ions and specific side functional groups plays an important role in the hydrolysis degradation process.

To further interrogate the efficacy of DHTE in the promotion of PET hydrolysis, we conducted a comprehensive series of depolymerization experiments varying the DHTE content and temperature with no added catalyst. As shown in Table 4 and Tables S1 and S2; Figure 6b, the 8 h degradation conversion of PEDHT5 in pure water increased by about 50% for each  $10^\circ\text{C}$  increment from  $160$  to  $180^\circ\text{C}$ . Moreover, the rate constant of PEDHT5 shows a twofold increase every  $10^\circ\text{C}$ . A



nearly quantitative hydrolysis was carried out at 200 °C in 2 h in pure water. PET and other PEDHTs show similar trends of the conversion and rate constant with respect to temperature compared to those of PEDHT5.

Compared with the traditional chemolysis pathways, here the high activity of the TH-unit is key to PET depolymerization over modest time periods with truly catalytic quantities of catalyst. The rapid scission at TH-units releases shorter chain fragments, disintegrates large solid particles, which reduces the mass transfer limitations of solid state polyester hydrolysis. The effect of TH-unit composition at 170 °C and 8 h is presented in Table 4 and Tables S1 and S2, Supporting Information; Figure 6b. The degradation conversion increases from 16.3% to 59.6% on moving from 0 to 5 mol% DHTE, and 93.6 wt% at 20 mol% DHTE. A similar trend is observed in the depolymerization rate constant, which shows an increase of around 150% with every 5% increase in DHTE loading, illustrating that depolymerization is strongly dependent on DHTE content.

Besides landfills, an unfortunate final destination for PET waste is the ocean. Accordingly, an ideal PET copolymer would degrade to small molecules rather than microplastics over reasonable time scales. Sea water is rich in metallic ions, such as Na<sup>+</sup>, Mg<sup>2+</sup>, and Ca<sup>2+</sup>, which could act as natural catalysts for electronic destabilization of the polymer chain to facilitate the bond cleavage. Therefore, ocean chemistry could be considered in the design of bottle-grade PET as a triggering condition for hydrolysis. Here, the influence of sea water was investigated by using PEDHT5 and was compared to the results in pure water, as presented in Table 4 and Figure 6b. The results under the condition of 160 to 180 °C for 8 h were used for comparison. The range of degradation conversion increases between 1.2% to 11.5% in the presence of sea water with corresponding increases in rate constant. These results have proved that the efficiency of PEDHT degradation is better in sea water than that in pure water, which could be attributed to the multiple kinds of metal ions in sea water that coordinate with TH units to catalyze hydrolysis. This suggests that ocean-specific TH units could be designed to better capitalize on marine chemistry to create more environmentally-friendly materials if accidentally released into the ocean.

Based on the discussion of the rate constant and the degradation conversion mentioned above, we can conclude that DHTE is an effective trigger for breaking down the PET polymer chain. Nonetheless, to understand the role of TH unit in PET more deeply, the degradation kinetics of PEDHT copolymers with multiple compositions were investigated, as presented in Figure 6b. The activation energy for hydrolysis degradation is 225, 117, 137, and 193 kJ mol<sup>-1</sup> for PET, PEDHT5, PEDHT10, and PEDHT20 systems, respectively. The activation energy decreases by nearly 50% with the insertion of 5% DHTE loading, followed by an increasing trend along with DHTE content. This observation could be ascribed to two opposing effects: on one hand, TH units tend to reduce the activation energy owing to the coordination effect with metal ions. On the other hand, DHTE forms additional ester bonds through its phenolic group, which increases the activation energy due to the increased branch/crosslink density and associated reduction in chain mobility. At low DHTE loading (5%), the energy saved by the coordination effect exceeds the energy needed to

break the additional ester bonds. However, as DHTE loading keeps increasing (>10%), the energy needed to break the additional ester bonds keeps growing and finally overwhelms the energy saved by metal coordination effect. Therefore, low DHTE loading decreases activation energy due to the coordination effect, but passes through a minimum value due to the network formation thereafter. The pre-exponential factor (A), which implies the collision spots for the reaction, also showed a similar trend as that of activation energy, and the values were e<sup>57.4</sup>, e<sup>29.5</sup>, e<sup>35.2</sup>, and e<sup>51.4</sup> for PET, PEDHT5, PEDHT10, and PEDHT20, respectively (Figure S5, Supporting Information). The maximum value shown from PET could be due to the linear and unbranched chain structure, which allows water to go more deeply into the polymer and increase the reactive spots to proceed with the hydrolysis degradation. With DHTE, the permanent covalent network formed by cross-linking could suppress water penetration and decrease the hydrolysis reactive spots, favoring surface erosion. However, as more DHTE are introduced into the polymer, the value of pre-exponential factors increases, suggesting that any reduction in water ingress is overwhelmed by the increasing hydrolytic sensitivity from DHTE. Thus, the pre-exponential factor decreases initially, followed by an increasing trend thereafter. That these trade-offs could possibly be eliminated by using a non-phenolic TH cunit, like 2,5-dimethoxy terephthalic acid, since the methoxy functional group would likely be stable throughout the polymerization process.

To help visualize the permanence of plastics in the environment, we extrapolated the Arrhenius kinetic model to conditions representative of ambient marine environments based on the parameters shown in Figure 6. There are several complex phenomena involved in polymer degradation, including the change in specific surface area, reaction order, crystallinity, and other microplastic degradation mechanisms.<sup>[53]</sup> As an illustrative simplification, Table 5 neglects these features to show the extreme time scales over which even partial hydrolysis occurs in average surface water temperatures of different locations and seasons of the ocean. This perspective shows how drastically the TH-unit-mediated reduction in the activation energy affects depolymerization under such mild conditions. 50% PET degradation in the tropical zone of the Indian Ocean is from about four to ten times faster than the Pacific Ocean or Mediterranean Sea, indicating a wide range of PET degradation rates. In neat PET, the large times reinforce the resilience of this resin under ordinary conditions. In contrast, the PEDHT data suggest that depolymerization in a natural environment could be shorter by several orders of magnitude. Other factors like UV radiation, current/wave force, enzymes, and microbes could further accelerate depolymerization beyond the simple chemical process considered here.<sup>[53–60]</sup> In the case of PEDHT copolymers, the trend of the required time is similar to that of activation energy and pre-exponential factor. The time passes through a minimum in PEDHT5, which shows a significant decrease of 6 orders of magnitude compared to that of pure PET. Further optimization of TH content and chemical design may also prove to be effective, which is promising in that chemically recyclable and even potentially biodegradable PET copolymers functionally indistinguishable from legacy PET may be achievable.

**Table 5.** Time needed for modified PET hydrolysis degradation under simulated marine environment.<sup>[52]</sup>

Sample Code	Time needed [years] for hydrolysis degradation conversion up to [%] under tropical zone of Pacific Ocean (30 °C)		Time needed [years] for hydrolysis degradation conversion up to [%] under tropical zone of Indian Ocean (35° C)		Time needed [years] for hydrolysis degradation conversion up to [%] under warm season of Mediterranean Sea (27 °C)	
	50%	99%	50%	99%	50%	99%
PET	6.42 <sup>a)</sup> 10 <sup>9</sup>	4.26 <sup>a)</sup> 10 <sup>10</sup>	1.50 <sup>a)</sup> 10 <sup>9</sup>	9.99 <sup>a)</sup> 10 <sup>9</sup>	1.57 <sup>a)</sup> 10 <sup>10</sup>	1.04 <sup>a)</sup> 10 <sup>11</sup>
PEDHT5	1.73 <sup>a)</sup> 10 <sup>3</sup>	1.15 <sup>a)</sup> 10 <sup>4</sup>	8.15 <sup>a)</sup> 10 <sup>2</sup>	5.41 <sup>a)</sup> 10 <sup>3</sup>	2.75 <sup>a)</sup> 10 <sup>3</sup>	1.83 <sup>a)</sup> 10 <sup>4</sup>
PEDHT5*	8.11 <sup>a)</sup> 10 <sup>2</sup>	5.39 <sup>a)</sup> 10 <sup>3</sup>	3.95 <sup>a)</sup> 10 <sup>2</sup>	2.62 <sup>a)</sup> 10 <sup>3</sup>	1.26 <sup>a)</sup> 10 <sup>3</sup>	8.40 <sup>a)</sup> 10 <sup>3</sup>
PEDHT10	1.40 <sup>a)</sup> 10 <sup>4</sup>	9.32 <sup>a)</sup> 10 <sup>4</sup>	5.82 <sup>a)</sup> 10 <sup>3</sup>	3.87 <sup>a)</sup> 10 <sup>4</sup>	2.41 <sup>a)</sup> 10 <sup>4</sup>	1.60 <sup>a)</sup> 10 <sup>5</sup>
PEDHT20	8.07 <sup>a)</sup> 10 <sup>6</sup>	5.36 <sup>a)</sup> 10 <sup>7</sup>	2.32 <sup>a)</sup> 10 <sup>6</sup>	1.54 <sup>a)</sup> 10 <sup>7</sup>	1.74 <sup>a)</sup> 10 <sup>7</sup>	1.15 <sup>a)</sup> 10 <sup>8</sup>

<sup>a)</sup>PEDHT5 in seawater.

While these observations point toward the possibility of designing high-performance biodegradable plastics, we envision that the most immediate use of the TH concept would be to improve the practicality of chemical recycling. Recent life cycle assessments of bottle-to-bottle PET recycling via enzymatic hydrolysis clearly show the severe impacts associated with the use of catalysts.<sup>[29]</sup> In the enzymatic process, the overall energy requirement was estimated to be about 74 MJ kg<sup>-1</sup>, comparing favorably with a 127 MJ kg<sup>-1</sup> expense for virgin PET bottles. However, it was found that as high as 57% of the embodied energy and other impact factors were associated with additional chemicals like NaOH and purification steps like TPA recrystallization. Additionally, Uekert et al. estimate that these purification steps involve 20–30% material losses, reducing the number of product lifetimes supported by the process. The internally catalyzed TH copolymers will eliminate these catalyst-related material and energy requirements, for example to as low as 32 MJ kg<sup>-1</sup> for recycled PET bottles.<sup>[29]</sup> Furthermore, TH copolymer hydrolysis may be more tolerant of contaminated feedstocks, potentially simplifying the pretreatment phase of the recycling process. A detailed process model incorporating the TH depolymerization and recovery steps will be developed to provide a more rigorous analysis. This will further help researchers understand the improvement in the recycling processes in order to meet industrial-scale standards and reduce environmental impacts.

To facilitate objective comparisons amongst the various chemolytic processes in the absence of such detailed process analysis, Barnard et al. proposed a simplified set of heuristics to provide a rough scoring in terms of temperature, solvent use, catalyst use, or other material requirements<sup>[61]</sup>

$$\varepsilon = \frac{Y}{Tt} \quad (1)$$

$$E = \frac{\left( 0.1 \frac{m_{\text{solvent}}}{m_{\text{PET}}} + \frac{m_{\text{catalyst}}}{m_{\text{PET}}} + \frac{m_{\text{other subst}}}{m_{\text{PET}}} \right)}{Y \frac{MW_{\text{product}}}{MW_{\text{repeat unit}}}} \quad (2)$$

$$\xi = \frac{E}{\varepsilon} \quad (3)$$

where  $\varepsilon$  is the “energy economy coefficient,”  $E$  is the “environmental factor,”  $\xi$  is the “environmental energy impact factor,”  $t$  is the depolymerization time (min),  $T$  is the reaction temperature (°C),  $Y$  is the fractional TPA/DMT/BHET mass yield,  $m_i$  is the mass of component  $i$ , and  $M_w$  is molecular weight.

$\varepsilon$  is a measure of the energy consumption of the depolymerization process, exclusive of any up- or down-stream processing, while  $E$  is related to the material requirements, and  $\xi$  is the ratio of these. To a first approximation, smaller  $E$ , smaller  $\xi$ , and larger  $\varepsilon$  values are associated with better material and energy efficiency. We applied these heuristics to PEDHT hydrolysis and several other PET chemolytic processes reported in the literature, as shown in Table S4 and Figure S8, Supporting Information. The low values of  $E$  and  $\xi$  are observed as a consequence of the usage of TH counits, compared to other traditional chemical recycling processes. Moreover, the representative environmental energy impact factor  $\xi$  of TH-aided depolymerization shows a decrease of over 90% compared to that of pure PET. This result indicates that this novel strategy is a promising one toward the direct depolymerization of PET polymer chain in solely water-based system with excellent energy economy.

### 3. Conclusions

In this work, PET incorporated with bioderived diphenolic TPA counits was successfully synthesized by a two-step polycondensation reaction. FTIR analysis revealed that trend of DHTE loading in the copolymers was consistent with the change in ratio of absorption intensity, and the phenolic group reacted with hydroxy ester group of the monomer and polymer chain to form the permanent covalent network. Based on the investigation on multiple reaction parameters, including catalyst concentration, hydrolysis time/temperature, and DHTE loading, the hydrolytic degradation of PEDHT copolymers with dilute metal catalytic aqueous solution can proceed easily under far milder conditions with no emission of toxic substances compared to traditional PET hydrolysis. Herein, the effect that DHTE imposed on degradability behaviors was the key to the improvement of PET chemical recycling. According to the hydrolysis kinetic data, the solid state degradation of PEDHT copolymers is first-order. DHTE destabilizes the chemical resilience of PET, where PEDHT5 showed the most rapid depolymerization rate.

Simple extrapolation of the Arrhenius kinetic model to ambient temperatures suggests an increase in the speed of PEDHT5 degradation by almost 6 orders of magnitude compared to neat PET. Moreover, the low values of  $E$  and  $\xi$  in the energy model show that this strategy has good energy economy in pure water system free of organic solvent and added catalyst.

The proposed mechanism of PEDHT hydrolysis degradation involves interactions between backbone ester bonds, ortho-substituted DHTE esters, and the metal ions, which result in the formation of a chelate. This coordination effect promotes the reactivity of the ester bonds in the polymer toward being attacked by the hydroxide ion of the water molecule, which facilitates depolymerization. Post depolymerization, the reclaimed solid products are two precursors (TPA and DHTE) and BHET dimer, which could be easily separated from water, and could further be regenerated into brand new polymer without performance deterioration. Furthermore, the thermal properties of PEDHT copolymers showed slightly higher  $T_g$  (4–7 °C) than that of PET, due to the increased energy barrier for the chain motion of the permanent covalent network in the amorphous domain. The suppression effect on the crystal thickness caused by the comonomer unit leads to  $T_m$  depression, indicating the potential to improve processibility. In the case of mechanical performance, the 3D network reinforced the rigidity of the copolymers, including Young's modulus, yield strength, and plastic deformation strength, but also caused the elongation at break to decrease along with increasing DHTE loading. These results suggest that DHTE is not only capable of being used for modifying PET degradability, but also conserves the thermal performance and is able to tune the mechanical properties of the materials to match requirements for the specific application.

In summary, this work provides a new strategy for PET chemical recycling while potentially maintaining full functional equivalency and compatibility with legacy PET. Moreover, the TH chemical used for polymer synthesis can be derived from biobased SA and the overall degradation procedure is environmentally friendly compared to those traditional approaches since water is the only needed material. Further studies including toxicology, techno-economic and life-cycle assessment, and gas barrier aspects, will be needed to provide a more comprehensive understanding of these materials before they are ready for end-use applications like food packaging.

## 4. Experimental Section

**Materials:** TPA (99+%, Acros Organics), EG (anhydrous, 99.8%, Sigma-Aldrich), and DHTE (97%, Oakwood Chemical) were used as precursors in polymer synthesis. Zinc acetate ( $Zn(CH_3COO)_2$ ), anhydrous, 99.8%, Alfa Aesar) and antimony(III) oxide ( $Sb_2O_3$ , 99%, Sigma-Aldrich) were respectively used as catalysts in the esterification/transesterification and polycondensation reactions. Triphenyl phosphate ( $\geq 99\%$ , Sigma-Aldrich) was used as a thermal stabilizer in the polycondensation reaction. Sea water (Imagitarium, Pacific Ocean Water) and zinc chloride ( $ZnCl_2$ , anhydrous, 98+%, Thermo Scientific) were used to study the degradation efficiency in a simulated marine environment. The product is natural sea water that is already filtered, sanitized, and pH balanced. Solvents and chemical reagents for analysis, such as dimethyl sulfoxide-d (DMSO-d), trifluoroacetic acid (TFA-d), chloroform-d ( $CDCl_3$ , 1 v/v% TMS), and pyridine (GCMS solvent) were

purchased from Fisher and used as received. N,O-bis(trimethylsilyl)trifluoroacetamide with 1% trimethylchlorosilane was purchased from Sigma-Aldrich and used as received.

**Synthesis:** PEDHT copolymers and pure PET were synthesized according to a classic two-step polycondensation reaction, as shown in Figure 2. Two-step polymerization was performed in a stainless-steel reactor (Parr Instrument Company, type 4560). The first step involved the esterification and transesterification of TPA and DHTE with EG, respectively, using zinc acetate (0.13% molar ratio relative to diester/diacid) as the esterification/transesterification catalyst. Diacid/diester and EG were charged into the autoclave reactor at a molar ratio of 1:10. The system was then purged with argon for 30 min, followed by increasing the reaction temperature up to 220 °C for 5 h with the pressure at 110 psi and an argon sweep to remove the byproducts (water and ethanol). Agitation was provided by a stainless-steel impeller at 250 rpm. After the first step reaction, the bis-hydroxy monomers and excess EG were transferred to a round-bottom flask for the distillation of EG using an oil bath set to 110 °C under vacuum for 12 h. The monomers were brought back to the autoclave reactor with antimony(III) oxide (0.02% molar ratio relative to the diacid/diester) and triphenyl phosphate (0.1% molar ratio relative to the diacid/diester) acting as catalyst and thermal stabilizer, respectively. The second step of polycondensation was carried out at 240 °C under high vacuum with the stirring speed set at 600 rpm to produce polymer. At the end of the reaction, the pressure was returned to ambient pressure using argon to prevent thermal oxidation of the product. The polymers were scraped out from the reactor followed by drying under vacuum at room temperature for 24 h.

**Polymer Degradation Procedure:** The general degradation procedure of the polymers is as follows:  $ZnCl_2$  and  $H_2O$  were mixed in a 100 mL glass liner in the desired ratio and stirred for 5 min. (1 and 0.1 wt%  $ZnCl_2$  solutions were prepared by weighing 0.3 and 0.03 g of  $ZnCl_2$ , respectively; then added DI water up to 30 g. Other concentrations followed the same procedure. 100% sea water purchased from Imagitarium was used to simulate marine environment) A transparent  $ZnCl_2/H_2O$  solution was formed followed by adding 1 g of PET or PEDHT powder after cryogrinding (Retsch). The liner was placed into a stainless-steel reactor (Parr Instrument Company, type 4560). The reactor was purged with argon gas and the inner pressure was increased up to 300 psi in order to keep the water in the liquid state during reaction. The reactor was heated and the starting point of the reaction was defined as reaching the set point of the target temperature. After the required reaction time, the reactor was removed from the heating mantle and cooled rapidly back to room temperature. The degradation products were filtered with quantitative filter paper (Whatman, ashless Grade 42) followed by two water washings. The remaining polymer and the precipitated monomers were recovered as solids due to poor solubility at room temperature, whereas EG was filtered as the liquid product. The reclaimed solid products were dried in a vacuum oven at 60 °C for 24 h. The dried products were weighed and analyzed by using  $^1H$  NMR to study the chemical structure and to evaluate PET conversion. GC-MS was further used to identify the composition and the purity of the solid products.

**Characterization:** Chemical structures were analyzed by using solution  $^1H$  NMR spectroscopy (Bruker Avance III 600 MHz spectrometer). DMSO-d was used for analysis of the solid products, while  $CDCl_3$  and TFA-d (75/25 v/v) solvent mixtures were used for degradation kinetic study.

The composition and the purity of the solid products were quantified by using an Agilent 6890 GC coupled with an Agilent 5975C MS detector. Chromatographic separation was performed by using an Agilent DB-1 column.

The functional groups of the copolymers were analyzed by FTIR (iD7 ATR Accessory for the Nicolet iS 5 Spectrometer, ThermoFisher). The spectra were obtained from 4000 to 400  $cm^{-1}$  from 32 scans at a resolution of 4  $cm^{-1}$ .

Due to crosslinking between the phenolic hydroxy of DHTE and terephthalate, swelling tests were used to determine the insoluble fraction in the copolymers. 150 mg of copolymer powder was immersed in a solvent mixture of phenol/1,1,2,2-tetrachloroethane (60/40 v/v) for

16 h at 120 °C. The gel was carefully filtered by membrane filter (0.22 μm pore size, hydrophobic PTFE, 47 mm membrane, MilliporeSigma) from the solution, washed in chloroform for 24 h, dried at 50 °C for 16 h under vacuum, and weighed.

Molecular weight and dispersity of the soluble fraction were determined using a Tosoh Ecosec GPC (Tosoh Ecosec HLC-8320GPC) equipped with a UV and RI detector. HFIP and DCAA (50/50 v/v) were used to dissolve the samples at a concentration of 6 mg mL<sup>-1</sup>. HFIP was used as the eluent at a flow rate of 0.3 mL min<sup>-1</sup>. The molecular weights were determined relative to poly(methyl methacrylate) standards.

Thermal properties of polymers were analyzed by using DSC (TA instruments Discovery DSC Q2500) under N<sub>2</sub> atmosphere. The samples were made by injection molding in order to study glass transition and crystallization behaviors. The samples were heated from 25 to 300 °C at a rate of 10 °C min<sup>-1</sup>, where they were held for 5 min before being cooled back to 25 °C at a rate of 10 °C min<sup>-1</sup>. The glass transition, crystallization, and melting temperature were obtained by using "Trios" software of TA Instruments. The thermal stability of the polymers was evaluated by TGA (STA 449 F1 Jupiter, NETZSCH). For each experiment, 5–6 mg of the samples in alumina crucible pan were heated from 80 to 1000 °C at a rate of 10 °C min<sup>-1</sup> under N<sub>2</sub> atmosphere.

Tensile specimens following the ISO 527-2 standard were prepared via injection molding (HAAKE Minijet, ThermoFisher) at 270 °C into a 40 °C mold. Tensile tests were conducted on an Instron 3369 at room temperature with a 1 kN load cell at a crosshead speed of 10 mm min<sup>-1</sup>. The dimension of the tensile bar is type 1BB with 2 mm (thickness) × 10 mm (gauge length).

The factors of hydrolysis degradation including catalyst concentration, temperature, reaction time, and copolymer composition, which affect the efficiency of the reaction, were identified. The degradation kinetics in various reaction conditions were also studied to clarify the roles of these factors. In the hydrolysis depolymerization kinetics of PET, the reaction order was usually considered pseudo-first-order since water is in excess over PET.<sup>[24,62,63]</sup> As a result, the TH-induced copolymer hydrolysis in the presence of metal catalyst was initially assumed to be controlled by the pseudo-first-order kinetic equation

$$\text{Rate} = kC_{\text{H}_2\text{O}}C_p = kC_p \quad (4)$$

where  $k$  is the rate constant and  $C_p$  is the concentration of PEDHT copolymer at time  $t$ .

$$C_p = C_{p0}(1-X) \quad (5)$$

where  $X$  is PEDHT copolymer hydrolysis conversion. Then, Equation (4) could be converted as follows

$$\frac{d(X)}{dt} = k(1-X) \quad (6)$$

Equation (6) was integrated over time to give Equation (7)

$$\ln \frac{1}{(1-X)} = kt \quad (7)$$

By using the rate constants, the activation energy  $E_a$  is obtained from Arrhenius Equation (8)

$$k = A e^{-\frac{E_a}{RT}} \quad (8)$$

Take the natural logarithm of both sides and get

$$\ln k = \ln A - \frac{E_a}{RT} \quad (9)$$

where  $A$  is the pre-exponential factor which corresponds to the collision frequency,  $R$  is the gas constant (8.314 J K<sup>-1</sup> mol<sup>-1</sup>), and  $T$  is the temperature in Kelvin. By using Equation (9), the rate constant at different temperatures can be calculated and further used in Equation (7) to estimate the time required for PET degradation to a certain degree.

**Statistical Analysis:** Data collected for this work were used without transformation. With the exception of tensile data in Table 3, tabulated values are single-point measurements. Table 3 values show mean and standard deviation mechanical properties derived from three repetitions.

Depolymerization experiments were fit to a first-order kinetic model using least-squares regression using Origin Pro software.

## Supporting Information

Supporting Information is available from the Wiley Online Library or from the author.

## Acknowledgements

The authors thank Sarah Cady (staff member at the ISU Chemical Instrumentation Facility) for training and assistance on the Bruker 600MHz NMR. The authors would also like to thank Lucas Showman (staff member of the W. M. Keck Metabolomics Research Laboratory) for training and assistance on the Agilent GC-MS. The authors acknowledge financial support from the Center for Bioplastics and Biocomposites (DMR-1626315) and the U.S. Department of Energy's Office of Energy Efficiency and Renewable Energy (EERE) under the Bioenergy Technologies Office Award Number DE-EE0009294. This report was prepared as an account of work sponsored by agencies of the United States Government. Neither the United States Government nor any agency thereof, nor any of their employees, makes any warranty, express or implied, or assumes any legal liability or responsibility for the accuracy, completeness, or usefulness of any information, apparatus, product, or process disclosed, or represents that its use would not infringe privately owned rights. Reference herein to any specific commercial product, process, or service by trade name, trademark, manufacturer, or otherwise does not necessarily constitute or imply its endorsement, recommendation, or favoring by the United States Government or any agency thereof. The views and opinions of authors expressed herein do not necessarily state or reflect those of the United States Government or any agency thereof.

Open access funding provided by the Iowa State University Library.

## Conflict of Interest

The authors declare no conflict of interest.

## Author Contributions

E.C. and G.K. conceived the idea and designed the study. T-H.L. carried out the polymer synthesis and degradation and other characterizations. M.F., T-p.W., H.L., and W.L. discussed the results and contributed to the experiment setup. D.D., L.S., and B.K. carried the thermal analysis and NMR characterization. T-p.W. and L.S. carried the mechanical testing. All authors contributed to writing and editing the manuscript.

## Data Availability Statement

The data that support the findings of this study are available from the corresponding author upon reasonable request.

## Keywords

biobased chemical, green recycling, low-energy poly(ethylene terephthalate) (PET) chemical recycling, neighboring group participation, poly(ethylene terephthalate) (PET) hydrolysis, poly(ethylene terephthalate) (PET)

Received: November 2, 2022

Revised: February 4, 2023

Published online:

- [1] E. K. Liu, W. Q. He, C. R. Yan, *Environ. Res. Lett.* **2014**, *9*, 091001.
- [2] M. Shen, B. Song, G. Zeng, Y. Zhang, W. Huang, X. Wen, W. Tang, *Environ. Pollut.* **2020**, *263*, 114469.
- [3] V. K. McElheny, *The New York Times* <https://www.nytimes.com/1977/04/13/archives/technology-the-dispute-over-plastic-bottles-technology.html> (accessed: April 1977).
- [4] M. Hestin, A. Mitsios, S. A. Said, F. Fourret, A. Berwald, V. Senlis, *Deloitte Sustainability: Blueprint for plastics packaging waste: Quality sorting & recycling* **2017**, <https://www2.deloitte.com/content/dam/Deloitte/my/Documents/risk/my-risk-blueprint-plastics-packaging-waste-2017.pdf>.
- [5] Global polyethylene terephthalate (pet) resin market to boost in coming years – projected to reach worth 114.7 million tons in 2028, <https://www.globenewswire.com/en/news-release/2022/04/04/2415938/0/en/Global-Polyethylene-Terephthalate-PET-Resin-Market-to-Boost-in-Coming-Years-Projected-to-Rreach-Worth-114.7-Million-Tons-in-2028-BlueWeave-Consulting.html> (accessed: April 2012).
- [6] I. Agenda, in *The New Plastics Economy Rethinking the future of plastics*, The World Economic Forum, Geneva **2016**, p. 36.
- [7] GA Circular, Full Circle: Accelerating the Circular Economy for Post-Consumer PET Bottles in Southeast Asia, **2019**, <https://drive.google.com/file/d/1LweI36tvAdad7ph6b4hHnL3C2nJ9rgmm/view>.
- [8] A. Al-Sabagh, F. Yehia, G. Eshaq, A. Rabie, A. ElMetwally, *Egypt. J. Pet.* **2016**, *25*, 53.
- [9] J. Hopewell, R. Dvorak, E. Kosior, *Philos. Trans. R. Soc. B: Biol. Sci.* **2009**, *364*, 2115.
- [10] N. George, T. Kurian, *Ind. Eng. Chem. Res.* **2014**, *53*, 14185.
- [11] S. Baliga, W. T. Wong, *J. Polym. Sci., Part A: Polym. Chem.* **1989**, *27*, 2071.
- [12] M. Imran, D. H. Kim, W. A. Al-Masry, A. Mahmood, A. Hassan, S. Haider, S. M. Ramay, *Polym. Degrad. Stab.* **2013**, *98*, 904.
- [13] A. Al-Sabagh, F. Yehia, A. Eissa, M. Moustafa, G. Eshaq, A. Rabie, A. ElMetwally, *Polym. Degrad. Stab.* **2014**, *110*, 364.
- [14] D. S. Achilias, H. H. Redhwi, M. N. Siddiqui, A. K. Nikolaidis, D. N. Bikiaris, G. P. Karayannidis, *J. Appl. Polym. Sci.* **2010**, *118*, 3066.
- [15] M. Parrott, WO2017087752A1, **2020**.
- [16] B. Shojaei, M. Abtahi, M. Najafi, *Polym. Adv. Technol.* **2020**, *31*, 2912.
- [17] H. Kurokawa, M.-a. Ohshima, K. Sugiyama, H. Miura, *Polym. Degrad. Stab.* **2003**, *79*, 529.
- [18] B.-K. Kim, G.-C. Hwang, S.-Y. Bae, S.-C. Yi, H. Kumazawa, *J. Appl. Polym. Sci.* **2001**, *81*, 2102.
- [19] M. J. Kang, H. J. Yu, J. Jegal, H. S. Kim, H. G. Cha, *Chem. Eng. J.* **2020**, *398*, 125655.
- [20] J. R. Campanelli, M. Kamal, D. Cooper, *J. Appl. Polym. Sci.* **1993**, *48*, 443.
- [21] G. Güçlü, T. Yalçınıyuva, S. Özgümüş, M. Orbay, *Thermochim. Acta* **2003**, *404*, 193.
- [22] S. D. Mancini, M. Zanin, *Polym.-Plast. Technol. Eng.* **2007**, *46*, 135.
- [23] G. Karayannidis, A. Chatziavougoustis, D. Achilias, *Adv. Polym. Technol* **2002**, *21*, 250.
- [24] Y. Wang, Y. Zhang, H. Song, Y. Wang, T. Deng, X. Hou, *J. Cleaner Prod.* **2019**, *208*, 1469.
- [25] M. E. Viana, A. Riul, G. M. Carvalho, A. F. Rubira, E. C. Muniz, *Chem. Eng. J.* **2011**, *173*, 210.
- [26] K. R. Delle Chiaie, F. R. McMahon, E. J. Williams, M. J. Price, A. P. Dove, *Polym. Chem.* **2020**, *11*, 1450.
- [27] J.-W. Chen, L.-W. Chen, *J. Appl. Polym. Sci.* **1999**, *73*, 35.
- [28] A. Launay, F. Thominet, J. Verdu, *Polym. Degrad. Stab.* **1994**, *46*, 319.
- [29] T. Uekert, J. S. DesVeaux, A. Singh, S. R. Nicholson, P. Lamers, T. Ghosh, J. E. McGeehan, A. C. Carpenter, G. T. Beckham, *Green Chem.* **2022**, *24*, 6531.
- [30] T.-H. Lee, H. Yu, M. Forrester, T.-p. Wang, L. Shen, H. Liu, J. Li, W. Li, G. Kraus, E. Cochran, *ACS Sustainable Chem. Eng.* **2022**, *10*, 2624.
- [31] K. Bowden, *Adv. Phys. Org. Chem.* **1993**, *28*, 171.
- [32] A. Kaplan, W. Sawodny, *Inorg. Chim. Acta* **1987**, *134*, 279.
- [33] G. N. Short, H. T. Nguyen, P. I. Scheurle, S. A. Miller, *Polym. Chem.* **2018**, *9*, 4113.
- [34] H. Liu, T.-H. Lee, Y. Chen, E. Cochran, W. Li, *ChemElectroChem* **2021**, *8*, 2817.
- [35] H. Liu, T.-H. Lee, Y. Chen, E. W. Cochran, W. Li, *Green Chem.* **2021**, *23*, 5056.
- [36] M. Okada, *Prog. Polym. Sci.* **2002**, *27*, 87.
- [37] J. P. Coates, P. H. Shelley, *Encyclopedia of Analytical Chemistry: Applications, Theory and Instrumentation*, Wiley, New York **2006**.
- [38] D. Montarnal, M. Capelot, F. Tournilhac, L. Leibler, *Science* **2011**, *334*, 965.
- [39] M. Capelot, D. Montarnal, F. Tournilhac, L. Leibler, *J. Am. Chem. Soc.* **2012**, *134*, 7664.
- [40] P. Carter, J. L. Trettin, T.-H. Lee, N. L. Chalgren, M. J. Forrester, B. H. Shanks, J.-P. Tessonier, E. W. Cochran, *J. Am. Chem. Soc.* **2022**, *144*, 9548.
- [41] S. Abdolmohammadi, D. Gansebom, S. Goyal, T.-H. Lee, B. Kuehl, M. J. Forrester, F.-Y. Lin, N. Hernández, B. H. Shanks, J.-P. Tessonier, E. W. Cochran, *Macromolecules* **2021**, *54*, 7910.
- [42] T.-H. Lee, H. Liu, M. J. Forrester, L. Shen, T.-p. Wang, H. Yu, J.-H. He, W. Li, G. A. Kraus, E. W. Cochran, *Macromolecules* **2022**, *55*, 7785.
- [43] P. C. Hiemenz, T. P. Lodge, *Polymer Chemistry*, CRC Press, Boca Raton, FL **2007**.
- [44] A. Demongeot, R. Groote, H. Goossens, T. Hoeks, F. Tournilhac, L. Leibler, *Macromolecules* **2017**, *50*, 6117.
- [45] D. Achilias, G. Karayannidis, *Water, Air, Soil Pollut.: Focus* **2004**, *4*, 385.
- [46] N. D. Pingale, V. S. Palekar, S. Shukla, *J. Appl. Polym. Sci.* **2010**, *115*, 249.
- [47] K. Li, X. Song, D. Zhang, *J. Appl. Polym. Sci.* **2008**, *109*, 1298.
- [48] K. Fukushima, O. Coulembier, J. M. Lecuyer, H. A. Almegren, A. M. Alabdulrahman, F. D. Alsewaillem, M. A. Mcneil, P. Dubois, R. M. Waymouth, H. W. Horn, J. E. Rice, J. L. Hedrick, *J. Polym. Sci., Part A: Polym. Chem.* **2011**, *49*, 1273.
- [49] H. Wang, Z. Li, Y. Liu, X. Zhang, S. Zhang, *Green Chem.* **2009**, *11*, 1568.
- [50] J. Sun, D. Liu, R. P. Young, A. G. Cruz, N. G. Isern, T. Schuerg, J. R. Cort, B. A. Simmons, S. Singh, *ChemSusChem* **2018**, *11*, 781.
- [51] S. Mattsson, M. Dahlström, S. Karlsson, *Tetrahedron Lett.* **2007**, *48*, 2497.
- [52] World sea temperatures, <https://www.seatemperature.org/>, (accessed: March 2023)
- [53] A. Chamas, H. Moon, J. Zheng, Y. Qiu, T. Tabassum, J. H. Jang, M. Abu-Omar, S. L. Scott, S. Suh, *ACS Sustainable Chem. Eng.* **2020**, *8*, 3494.
- [54] S. Yoshida, K. Hiraga, T. Takehana, I. Taniguchi, H. Yamaji, Y. Maeda, K. Toyohara, K. Miyamoto, Y. Kimura, K. Oda, *Science* **2016**, *351*, 1196.
- [55] R. Koshti, L. Mehta, N. Samarth, *J. Polym. Environ.* **2018**, *26*, 3520.
- [56] R. Wei, W. Zimmermann, *Microb. Biotechnol.* **2017**, *10*, 1302.
- [57] D. Danso, C. Schmeisser, J. Chow, W. Zimmermann, R. Wei, C. Leggewie, X. Li, T. Hazen, W. R. Streit, *Appl. Environ. Microbiol.* **2018**, *84*, e02773.
- [58] B. Gewert, M. M. Plassmann, M. MacLeod, *Environ. Sci.: Processes Impacts* **2015**, *17*, 1513.
- [59] A. K. Urbanek, W. Rymowicz, A. M. Mirończuk, *Appl. Microbiol. Biotechnol.* **2018**, *102*, 7669.
- [60] C. P. Ward, C. M. Reddy, *Proc. Natl. Acad. Sci. U. S. A.* **2020**, *117*, 14618.
- [61] E. Barnard, J. J. R. Arias, W. Thielemans, *Green Chem.* **2021**, *23*, 3765.
- [62] D. Kim, B.-k. Kim, Y. Cho, M. Han, B.-S. Kim, *Ind. Eng. Chem. Res.* **2009**, *48*, 6591.
- [63] R. López-Fonseca, I. Duque-Ingunza, B. de Rivas, L. Flores-Giraldo, J. I. Gutiérrez-Ortiz, *Chem. Eng. J.* **2011**, *168*, 312.